European Spine Journal
https://doi.org/10.1007/s00586-025-09163-7

RESEARCH

Segmentation-based 3D volumetry and linear regression modeling for assessing the vertebral bone loss in pyogenic vertebral osteomyelitis

Siegmund Lang[1] · Michael Bachtler[1] · Josina Straub[1] · Jonas Krückel[1] · Susanne Baertl[1] · Melanie Ardelt[2,3] · Gerardo Napodano[4] · Michael Haimerl[5] · Markus Loibl[6] · Volker Alt[1] · Maximilian Kerschbaum[1]

Received: 16 May 2025 / Revised: 6 July 2025 / Accepted: 13 July 2025

Abstract

Background Pyogenic vertebral osteomyelitis (PVO) presents an escalating clinical challenge due to rising incidence, high mortality, and significant bone destruction. Objective quantification of vertebral body (VB) bone loss for assessing the disease severity and guiding therapeutic decisions is yet to be established.

Methods We retrospectively identified patients with confirmed PVO between 2010 and 2020. Volumetric assessments of VBs were performed using 3D Slicer, and pre-infection volumes were estimated by linear regression based on adjacent, non-infected vertebrae. A "Destruction Quotient" (DQ) was calculated (measured volume/estimated original volume) to quantify VB loss. In a subgroup analysis VB bone loss was evaluated, depending on sex, spinal location and pathogen group.

Results Thirty-one patients met the inclusion criteria for 3D volumetry (16 males, 15 females; mean age: 67.0 ± 9.2 years; mean BMI 32.4 kg/m²). In total, $n = 267$ VBs were segmented. Linear regression models demonstrated a high mean coefficient of determination ($R^2 > 0.95$), with mean slopes of m = 2.3 (95% CI = 1.94–2.75) in males and m = 1.8 (95% CI = 1.46–2.19) in females. The mean measured volume of infected VBs (17.8 ± 9.3 cm³) was significantly lower than the estimated original volume (24.1 ± 10.5 cm³; $p < 0.001$). VBs at the lumbar spine experienced a median volume loss of 30%, whereas thoracic VBs showed 18% loss of volume. Female patients demonstrated a significantly higher median VB loss (32%) than males (12%; $p < 0.05$). No significant variation in DQs was observed among different pathogen groups, with *Staphylococcus aureus* being the most prevalent; however, within the *Staphylococcus aureus* subgroup, the measured VB volume was significantly smaller than the original estimated volume with a mean difference of 6.13 ± 4.9 cm^3 ($p < 0.01$).

Conclusion A 3D-volumetric approach and linear regression modeling offers an individualized method for quantifying VB destruction in PVO. Integrating automated segmentation and densitometric data may further enhance predictive accuracy and improve patient-specific treatment strategies.

Keywords Spinal infections · Vertebral osteomyelitis · Spondylodiscitis · 3D-Volumetry · Segmentation

Introduction

Spinal infections, first and foremost pyogenic vertebral osteomyelitis (PVO) demonstrates a troubling increase in the incidence and mortality of vertebral osteomyelitis in Germany, with a significant impact on the aging population [1, 2]. The high in-hospital mortality rates of 2–13% pose a significant clinical challenge due to the potential for severe morbidity and spinal column instability [3, 4]. In addition to the impact of age, comorbidities, such as rheumatoid arthritis, congestive heart failure and kidney disease, have been strongly associated with an increased risk of mortality [4–6]. Beyond physical impairment, vertebral osteomyelitis can also lead to substantial mental disorders [7].

PVO is marked by the destruction of vertebral bodies (VB), potentially resulting in spinal instability, neurological deficits, and chronic pain [8]. Traditional PVO assessment depends on clinical evaluation, MRI, and CT, but lacks precise quantification of bone loss, limiting severity assessment and instability prediction. Several studies stress the need for accurate vertebral bone loss quantification. For instance, Limthongkul et al. demonstrated a quantitative

Extended author information available on the last page of the article

Published online: 26 July 2025

approach to vertebral body volume assessment using CT scans, showing significant variations in VB volumes along the thoracic and lumbar spine [9]. However, these studies lack a standardized method for estimating the original, pre-infection volumes of VB, which is essential for calculating the true extent of bone destruction in infected vertebrae [9, 10]. Advancements in three-dimensional (3D) imaging and open-source software tools, such as 3D Slicer, have opened new avenues for volumetric analysis of VB. These tools allow for the creation of detailed 3D models from CT scans, enabling more precise measurements of VB volumes and the ability to differentiate between infected and non-infected vertebrae [11, 12]. Accurate quantification of vertebral bone loss is clinically relevant, as it may reflect disease severity, support surgical decision-making, and aid in predicting spinal instability, particularly in infections involving weight-bearing segments.

This study aimed to use 3D volumetric analysis and linear regression modeling to quantify vertebral body destruction in PVO, establishing a reliable destruction quotient to assess disease severity, predict spinal instability, and guide surgical decisions. The goal is to create a robust framework for quantitative evaluation of bone loss in PVO.

Methods

Data analysis of pyogenic vertebral osteomyelitis patients

Patients diagnosed with PVO (ICD10: M46.1-4), treated conservatively or surgically at the University Hospital Regensburg between 2004 and 2020 were eligible for inclusion. Subsequently, adult patients' medical records, surgical protocols, laboratory results, and microbiological and histopathological reports were reviewed for criteria indicative of vertebral osteomyelitis (VO). The diagnosis of VO was established if at least two of the following criteria were met: (1) clinical features consistent with VO; (2) radiological evidence of vertebral osteomyelitis on CT and/or MRI [13, 14]; or (3) microbiological identification of bacterial pathogens, either directly from the infection site (e.g., abscess, intervertebral disc, or vertebral bone) or from blood cultures [15]. Furthermore, the records needed to contain a CT scan of the thoracolumbar spine.

CT-DICOM data set selection criteria

CT images were obtained from Siemens Healthineers' SOMATOM Definition Flash and Go Top systems. The Flash offers high-speed, low-radiation dual-source imaging, while the Go Top captures 128-slice scans, ideal for detail. For the logistic model, eligible scans had clear views of the affected vertebrae and four non-infected adjacent vertebrae, with minimal noise and slice thickness up to three millimeters.

3D slicer software

We utilized 3D Slicer, a robust, open-source platform for medical image analysis and visualization, to perform volumetric analysis of vertebral structures. 3D Slicer has become a standard tool in clinical research, medical education, and image-guided therapy due to its support for multimodal imaging (CT, MRI, PET) and extensive modular capabilities [16]. The software's accuracy in volume measurement is well-documented in peer-reviewed studies, confirming its reliability for clinical research [17, 18].

Application of 3D slicer for volume measurement

Initially, anonymized DICOM data was imported into 3D Slicer. The software's modular workflow facilitates a range of analyses, from preprocessing to quantitative assessment, and is optimized for reproducibility and customization. For this study, key modules were utilized to ensure precise volumetric analysis of vertebral structures:

Preprocessing and region of interest (ROI) definition

The "Crop Volume" module isolated the target vertebra, excluding posterior structures from the pedicles onward, ensuring efficient processing and precise segmentation.

Segmentation workflow

Using the Segment Editor module, individual vertebral bodies were segmented, with separate segments assigned for infected and non-infected vertebrae. All segmentations were performed by a single trained annotator under supervision of a board-certified spine surgeon. Random samples were reviewed for anatomical plausibility. Formal inter-observer variability assessment was not conducted and is acknowledged as a limitation. The segmentation process combined automated and manual tools for optimal precision:

- Thresholding: Hounsfield Unit (HU) thresholds, ranging from 150 to 250 HUs, were applied to isolate bone tissue from surrounding soft tissues. Threshold adjustments were subjectively fine-tuned for each scan to enhance contrast (Fig. 1).
- Grow from Seeds: This semi-automated tool extrapolated initial segmentation across the entire vertebral

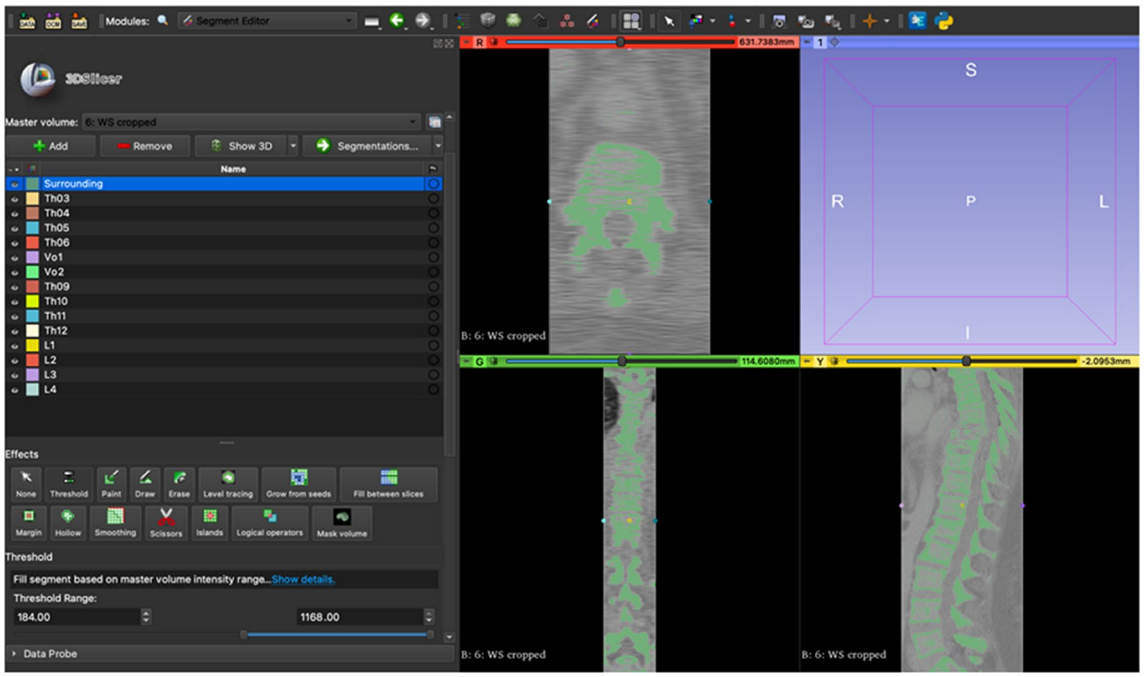

Fig. 1 3D Slicer workflow: Application of Hounsfield Unit thresholding to isolate bone tissue from surrounding soft tissues, with manual adjustments to optimize contrast for each scan

volume. Manual oversight was critical to ensure accurate propagation of the segmentation (Fig. 2).

Manual Refinements: Tools such as "Paint" and "Erase" were used to fine-tune segmentation, specifically excluding posterior elements like pedicles to focus solely on vertebral bodies (Fig. 3). Protruding osteophyte attachments were also removed in order to focus uniformly on the vertebral body as a cylindrical shape (Fig. 3B).Vertebrae with excessive bony overgrowth or spondylophytes that impaired clear boundary delineation were excluded from DQ analysis due to unreliable volumetric estimation.

Estimation of pre-infection volume of infected vertebral bodies

To assess vertebral body (VB) volume changes due to infection, pre-infection volumes ($V_{original}$) were estimated using linear regression analysis on non-infected VBs, yielding a coefficient of determination (^{2}) to confirm linearity. The simple regression model.

$$f(x) = m \cdot x + t$$

was applied to estimate the original volume of the infected VBs. Subsequently, the "Destruction Quotient" (DQ) was calculated to assess volume changes due to infection:

$$DQ = \frac{\text{Measured Volume of Infected VB (Vmeasured)}}{\text{Estimated Original Volume of Infected VB (Voriginal)}}$$

Values < 1 indicate volume loss and > 1 suggest volume gain. Patients with preexisting severe degeneration of the infected segment were excluded from the final evaluation of volume changes in vertebral osteomyelitis, as the high difficulty in segmenting vertebral body borders and differentiating between spondylophytes compromised the accuracy of measurements.

Statistical methods

Data analysis was conducted using SPSS Version 28. Parametric data were reported as mean ± SD, non-parametric data as median (Min–Max). Bootstrapped 95% CIs (2,000 samples, BCa method) were calculated. VB volume progression linearity was assessed via simple linear regression (^{2}). Normality was tested with Shapiro-Wilk. Parametric data were analyzed with t-tests, while Mann-Whitney U and Wilcoxon signed-rank tests were used for independent and paired non-parametric comparisons, respectively. Kruskal-Wallis tests compared multiple non-parametric groups, and Spearman's rho assessed correlations. Statistical significance was set at $p < 0.05$.

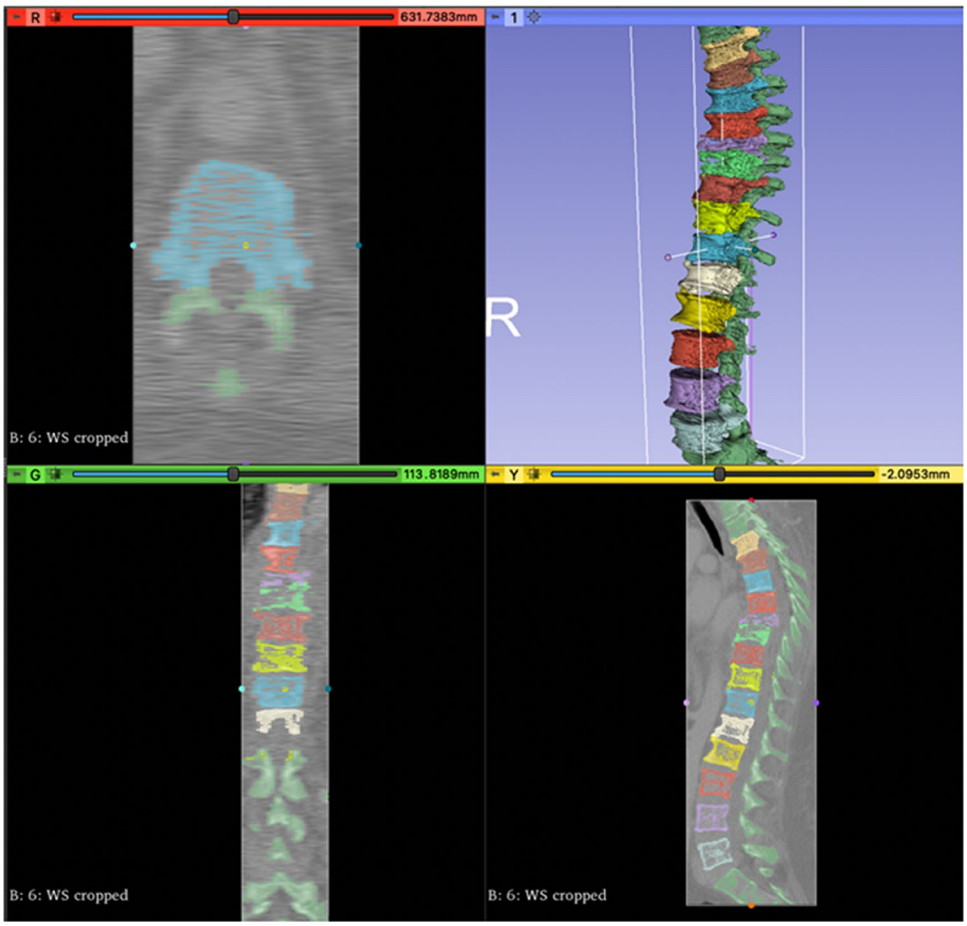

Fig. 2 Visualization of the spine in 3D Slicer. Three-dimensional reconstruction of the spine generated using the "Grow from Seeds" function within the 3D Slicer software, illustrating the segmentation process for vertebral bodies

Results

Patient characteristics

Out of $N=255$ eligible patients $n=61$ PVO patients were included. After applying the CT selection criteria, $n=31$ patients were deemed suitable for volumetric analysis (Fig. 4). The cohort comprised $n=15$ women (48.4%) and $n=16$ men (51.6%), with an average age of 67.0 ± 9.2 years. The mean BMI was 32.4 kg/m².

In $n=25$ (80.6%) cases pathogens were identified, with $n=4$ (19.4%) cases of polymicrobial infections. There were $n=6$ culture negative cases. Among the identified pathogens ($n=29$), Staphylococcus species were the most prevalent, accounting for $n=17$ (58.6%) cases, with *Staphylococcus aureus* (STAU) being the most frequent individual pathogen, identified in $n=13$ (44.8%) cases. Enterococci were the second most common Gram-positive group, representing $n=3$ (10.3%) cases. Gram-negative bacteria were identified in $n=6$ (20.7%) cases, with Enterobacteriaceae (including *Escherichia coli*, *Klebsiella pneumoniae*, *Citrobacter freundii* and *Enterobacter cloacae*) being the predominant subgroup ($n=5$). One *Pseudomonas aeruginosa* infection was documented. Overall, Gram-positive pathogens accounted for $n=23$ (79.3%) of infections, while Gram-negative pathogens represented $n=6$ (20.7%).

3D volumetry

$N=267$ VBs were measured with 3D volumetry. A total of $n=212$ non-infected VBs were measured, with an average volume of 21.2 cm³. The average volume of thoracic VBs was 17.8 cm³ and 30.7 cm³ for lumbar VBs. The average volume of each VB is given in Fig. 5.

Linearity assessment of vertebral volume data

The values used to assess linearity were derived from VB volume measurements from the studies by Limthongkul et al. and Molloy et al., as well as the data from this study. For the dataset from Limthongkul et al. [9], an R^2 of 0.96 was obtained for the spinal segment from Th01 to L4.The data from Molloy et al. [19] yielded an R^2 of 0.99 for the segment from Th06 to L4. With an R^2 of 0.95 for Th01–L4 and consistently high values across studies, vertebral body volume growth was assumed linear, justifying the applied regression model.

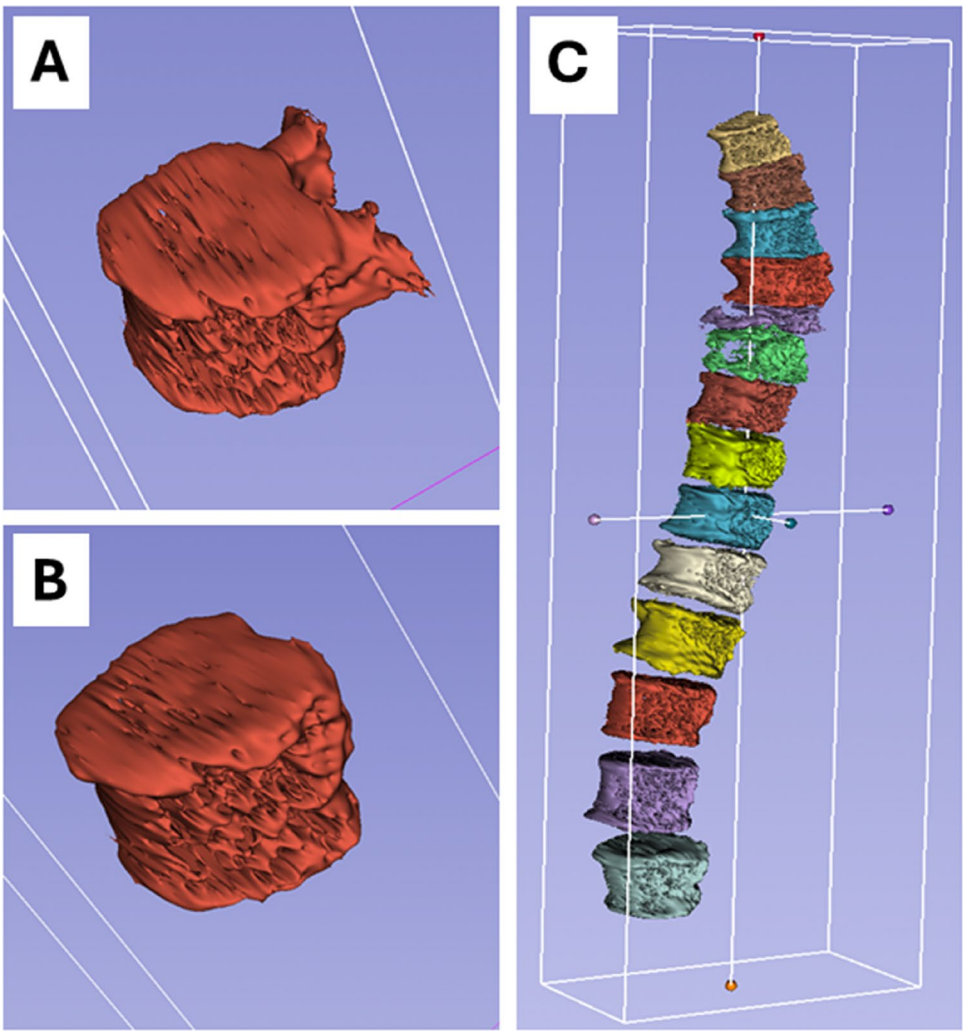

Fig. 3 Adjustment of a vertebral body (VB) segmentation in 3D Slicer using the "Erase" tool. The image illustrates the refinement process to meet defined criteria. (A) Initial segmentation; (B) Refined segmentation after adjustments. Example of a segmented spine following volume measurement in 3D Slicer. The 5th and 6th thoracic vertebral bodies from the top are identified as the infected segments, highlighted within the segmented model (C)

Linear regression model

The linear regression was conducted case by case and yielded in individual slopes (m). The mean slope for males was 2.3 ± 0.8 (95%CI = 1.94–2.75, Fig. 6A), while for females, it was 1.8 ± 0.7 (95%CI = 1.46–2.19, Fig. 6B).

Volume of the infected VBs

A methodical example is given in Fig. 7, that shows the individual regression model (() = 2.2*x + 3.0; $R^2 = 0.94$) of a patient with VO of Th9 and Th10.

Vertebral bodies at the lumbar spine (L1–L4) were affected 28 times by PVO, and at the thoracic spine (Th01–Th12) 27 times, giving a mean of n = 1.8 affected VBs per included patient. The most frequently affected VBs were L2 (9 cases), followed by L1 and L3 (7 cases each). For the detailed analysis, only the mainly affected VB of an infected segment was considered. Cases with severe degenerative deformation of the infected segment, marked by excess bone mass in spondylophytes and DQ > 1, were excluded from the final analysis as detailed in the methods.

This resulted in a sub-group of $n = 20$ PVO patients (female $n = 8$ and male $n = 12$), aged 67.1 ± 10.0 years and a mean BMI of 31.6 ± 6.2 kg/m². The mean calculated original volume ($V_{original}$) of these VBs was 24.1 ± 10.5 cm^3. The mean 3D-volumetric volume of these infected WBs was 17.8 ± 9.3 cm^3, giving a mean difference of 6.3 ± 5.0 cm^3 and a median DQ 0.81 (0.42–0.93). The average measured volume was significantly smaller than the calculated original volume ($p < 0.001$; Fig. 8).

At the thoracic spine the mean $V_{original}$ was 20.4 ± 8.3 cm^3 and the median loss of vertebral bone was 18% (7–57%). At the lumbar spine the mean calculated initial volume was 30.8 ± 10.3 cm^3 and the median loss of vertebral bone volume was 30% (11–58%). The mean, absolute difference between the calculated original Volume and the measured Volume was significantly higher at the thoracic spine (9.6 ± 6.1cm^3) compared to the lumbar spine (4.4 ± 2.6 cm^3; $p < 0.05$). A moderate, statistically significant positive

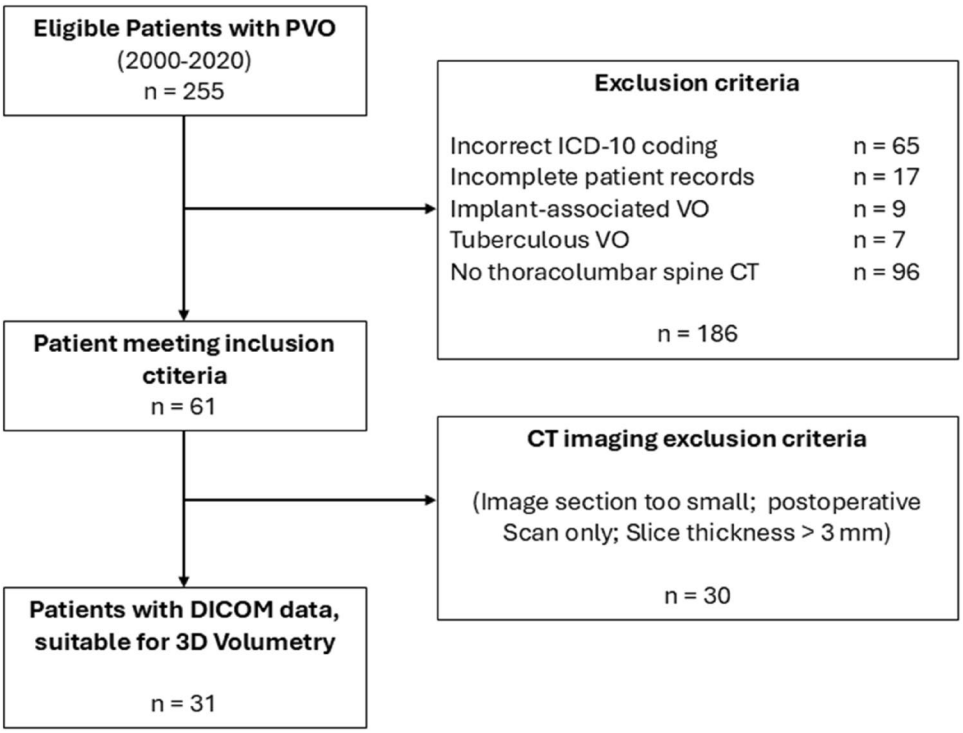

Fig. 4 Flowchart illustrating the inclusion and exclusion process for patients with PVO, resulting in 31 patients suitable for 3D volumetric analysis

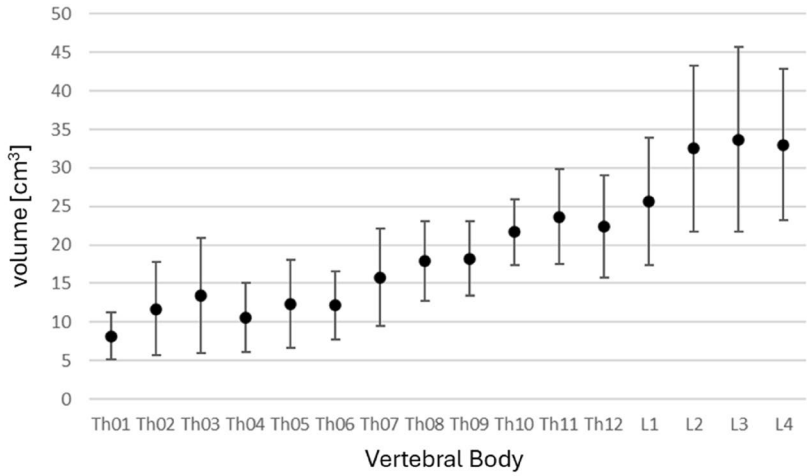

VB	Th01	Th02	Th03	Th04	Th05	Th06	Th07	Th08	Th09	Th10	Th11	Th12	L1	L2	L3	L4
Mean volume	8.2	11.7	13.4	10.6	12.4	12.2	15.8	17.9	18.2	21.7	23.6	22.4	25.6	32.5	33.7	33.0

Fig. 5 Mean and standard deviation of vertebral body volumes for all measured vertebrae

correlation of $\rho = 0.427$ between patient sex and the DQ was seen, with female patients loosing 32% (15–57%) of the original bone volume and male patient 12% (7–58%; median DQ male: 0.88 (0.42–0.98); median DQ female: 0.68 (0.43–0.85; $p < 0.05$).

While the lowest median DQ of 0.66 (0.65–0.89) was seen in patients with Gram-negative pathogens, the Kruskal-Wallis Test did not show a statistically significant difference between the 4 pathogen groups (STAU; other Gram-positive; Gram-negative; culture-negativfew; Fig. 9; $p > 0.05$). The median VB volume loss in patients with STAU was 19% ($n = 10$; 11–57%), in patients with other Gram-positive pathogens 26% ($n = 2$; 11–41%), in patients with Gram-negative pathogens 34% ($n = 3$; 11–35%) and in patients with negative cultures 12% ($n = 5$; 7–58%). However, only in patients with STAU there was a statistically significant difference between $V_{original}$ and $V_{measured}$ of 6.1 ± 4.9 cm^3 ($p < 0.01$).

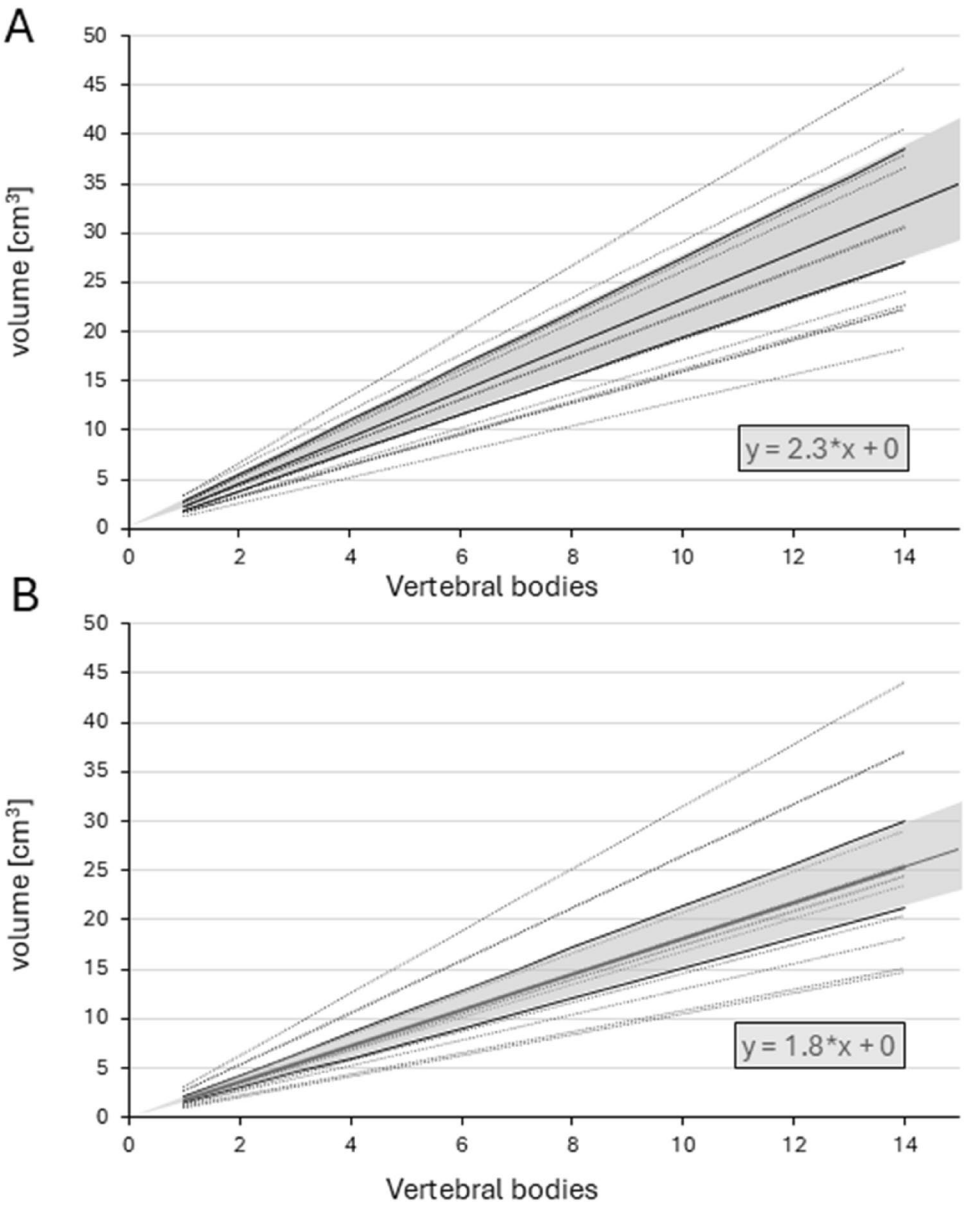

Fig. 6 Linear regression slopes for male (**A**) and female patients (**B**), presented as functions shown as dotted trendlines. The grey areas represent the 95% Confidence intervals. The central line within the 95%CIs represents the mean slope with x-axis-section (t) = 0

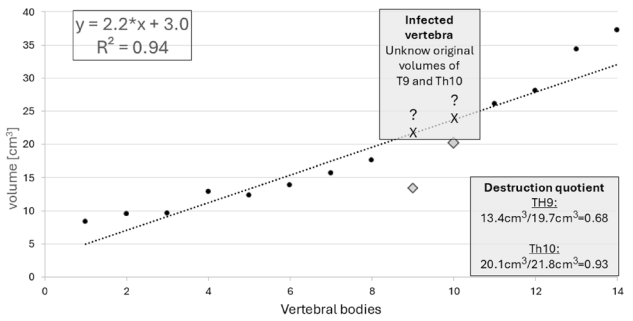

Fig. 7 Example case of a patient with PVO of Th9 and Th10. Although unknown, given the individual equation, the original volume, $V_{original}$ of the two infected VBs was estimated ($V_{original\_Th9}$ = 19.7cm^3 and $V_{original\_Th10}$ = 21.8cm^3) and actual volumes were measured ($V_{measured\_Th9}$ = 13.4cm^3 and $V_{measured\_Th10}$ = 20.1cm^3), enabling calculation of the DQ in the subsequent step

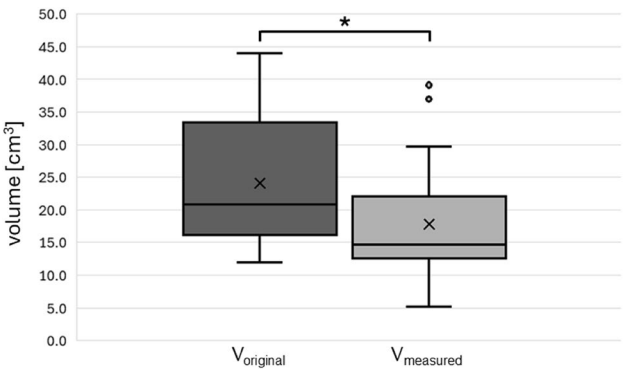

Fig. 8 Boxplots display the median (horizontal line), mean (x), interquartile range (25th–75th percentile), and minimum-maximum values (whiskers). Outliers are shown as individual points. The measured volume ($V_{measured}$) was significantly smaller than the original calculated volume ($V_{original}$; $p < 0.001$, *)

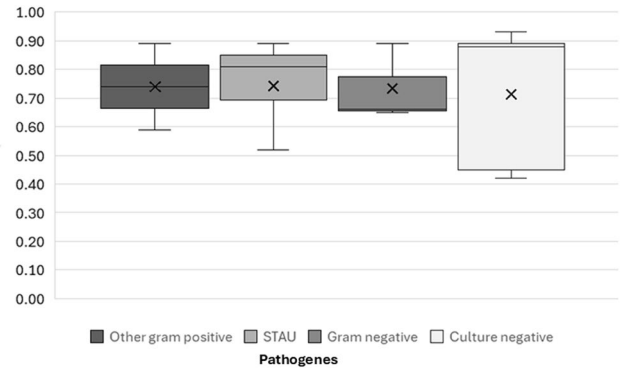

Fig. 9 Boxplots display the median (horizontal line), mean (x), interquartile range (25th–75th percentile), and minimum-maximum values (whiskers) for the DQs of different pathogen groups: Other Gram-positive, *STAU*, Gram-negative, and Culture-negative

Discussion

This study introduces, for the first time to the authors' knowledge, a patient-specific mathematical approach to estimate the original (pre-infection) vertebral body volume and quantify the extent of osteolytic lesions in PVO. By deriving a linear function based on the cranio-caudal increase in VB volumes and requiring only two accurately measured healthy VBs, the estimation of the "original" volume $V_{original}$ of an infected or otherwise affected vertebra is enabled.

Multiple studies, including those by Limthongkul et al. and Molloy et al., consistently demonstrate a near-linear increase in vertebral body (VB) volume from Th01 to L4, with high coefficients of determination (0.95–0.99) [9, 19]. Our results echo this trend, showing an $R^2 = 0.95$ for the mean volume of non-infected thoracolumbar VBs, thus reinforcing the linear growth model (Table 1). However, at L5 the literature indicates the linearity breaks off, likely due to anatomical and biomechanical variations; hence, simple linear regression is not reliably applicable at that level. Demographic differences in spinal anatomy must be considered, emphasizing the need for an individualized approach supported by suitable demographic data and highlighting the potential importance of big data integration. It must also be taken into account that the assumed linearity may be limited in patients with congenital anomalies, postoperative or degenerative changes.

Accurate bone volume estimation is crucial for diagnosis and treatment. In vertebroplasty or kyphoplasty, it helps determine the optimal bone cement volume for structural restoration [19]. This quantification is likewise valuable in the context of osteolytic diseases, including not only PVO but also metastatic tumor infiltration, where volumetric bone destruction necessitates robust classification systems and clearer indications for operative intervention [23]. By integrating an automatically derived bone volume DQ, more nuanced, patient-specific classifications could be developed, and prognostic accuracy could be increased.

Manual segmentation in open-source software, such as 3D Slicer, remains time-consuming and prone to interobserver variability [17, 24]. However, modern segmentation tools leverage artificial intelligence (AI) and advanced imaging algorithms to achieve near real-time volumetric analyses [11]. Chen et al. evaluated the accuracy and efficiency of Brainlab´s Elements SmartBrush Spine for autosegmenting clinical target volumes (CTV) in spine SBRT, showing high consistency and agreement with clinically used CTVs while reducing inter-person variation and contouring time [25]. Integrating the linear regression model into a software pipeline would potentially facilitate automated measurement of an adjacent healthy VB, application of the patient-specific equation, and generation of the DQ. This approach holds promise for integration into AI-based algorithms that can automatically detect vertebral fractures on routine CT scans [26]. Subtle volumetric changes or occult fractures could thus be flagged early, guiding clinicians to intervene in osteoporotic patients and those with multiple myeloma, metastatic lesions, or spinal infections.

Incorporating Houndsfield Units (HU) data could refine the model. Dieckmeyer et al. identified level-specific vBMD thresholds with opportunistic QCT, showing strong links between low vBMD and fracture risk [27]. Similarly, a combined volumetric-HU model could thus capture both the quantity and quality of lost bone mass,

Table 1 Comparison of vertebral volume measurement methods, sample sizes, and results

Study	Molloy et al., 2003 [19]	Odaci et al., 2003 [20]	Komemushi et al., 2009 [21]	Limthongkul et al., 2010 [22]	Caula et al., 2016 [23]	Current Study
Method	Archimedes' Principle	Cavalieri principle	CT -Volumetry	CT -Volumetry BrainLab	Cylinder: $V = \pi R$	CT Volumetry: 3D Slicer
Number of Patients/Vertebrae	10 P/120 VB	2 P/10 VB	8 P/104 VB	40 P/680 VB	129 P/645* VB	31 P/267 VB
Total Spine [cm³]	(from T6) 29.5	–	(from T5) 26.3	(excl. L5) 20	–	(excl. L5) 21.2
Thoracic Spine [cm³]	–	–	–	15	–	17.8
Lumbar Spine [cm³]	(incl. L5) 41	(incl. L5) 30.6	–	(excl. L5) 35.1	(excl. L5) 35.5	(excl. L5) 30.7

improving PVO patient risk stratification for collapse and other complications.

In the current cohort, there was no statistically significant difference in the DQ with respect to pathogen type. These subgroup comparisons should be interpreted with caution due to the small number of patients within each pathogen group, which may limit statistical power and generalizability. Nevertheless, only in patients with STAU infection the differences between $V_{original}$ *and* $V_{measured}$ were statistically significant. It is plausible that more aggressive organisms like the high-virulent STAU induce earlier or more extensive bone volume loss [28, 29]. Widaa et al. highlighted, that *Staphylococcus aureus* protein A plays a pivotal role in osteomyelitis by inducing bone destruction and bone loss through apoptosis of osteoblasts, inhibition of bone formation, and activation of osteoclasts via soluble RANKL secretion [28]. Coagulase-negative staphylococci (CONS), with *Staphylococcus epidermidis* exhibit lower virulence [3, 30]. They primarily play a role in chronic and implant-associated infections [31–33].

In fact, the lowest DQ of 0.66 and thus the highest amount of bone loss was seen in the group with Gram-negative pathogens. They are known to exhibit a moderate to high virulence and are associated with high mortality rates in PVO patients [5, 34]. Kang et al. found, that pyogenic spondylitis caused by Gram-negative bacteria was strongly associated with genitourinary and intra-abdominal infections, presenting more frequently with severe sepsis, but with similar mortality and clinical outcomes compared to Gram-positive cocci [35].

However, the factors for severe courses of disease in PVO are multifold [4, 5, 36]. The relationship between pathogen virulence, immune status, and bone health in vertebral osteomyelitis is complex [37, 38].

Integrating osteoimmunology and bone turnover differentiation may improve understanding and treatment. This study provides a framework for quantifying bone loss, with future research linking volumetric data to pathogen virulence and patient-specific turnover to elucidate infection-driven bone destruction.

All in all, this study could lay the foundation for assessing the severity of the course of the disease by determining the degree of destruction of an infected vertebral body at the time of diagnosis. From a clinical standpoint, the DQ may support surgical decision-making by identifying patients at risk of instability. It could serve as a longitudinal marker of structural deterioration and be integrated into predictive models to guide stabilization strategies or intensification of antimicrobial therapy. Correlation with bone metabolism biomarkers may improve understanding of infection-induced osteolysis. Beyond PVO, the approach may also be valuable in osteoporotic fractures and metastatic spinal disease. The volumetry could be a helpful tool in kyphoplasty planning to estimate the optimal volume of bone cement to be applied.

Limitations

This study is limited by its small sample size and retrospective design, which inherently restricts the generalizability of the findings. Additionally, the cases included CT scans taken at varying stages of disease progression and ongoing therapy, introducing heterogeneity in bone destruction and treatment effects. Furthermore, our regression-based model assumes a linear trend in vertebral body volume along the thoracolumbar spine. This assumption may not hold in patients with congenital anomalies, prior trauma, or advanced degenerative disease, potentially limiting the accuracy of the estimated pre-infection volumes. In addition, metal implants from prior spinal surgeries (e.g., pedicle screws) may create artifacts that impair segmentation accuracy and volumetric calculations. The primary aim was not to evaluate clinical outcomes or treatment modalities. Instead, the focus was on validating the feasibility of the linear regression model and its application in a series of 3D-segmented vertebral bodies, providing a foundation for future, standardized quantification of bone volume loss in pyogenic vertebral osteomyelitis. Future multicenter studies are warranted to validate the robustness and applicability of this method in more diverse patient populations.

Conclusion

We introduce patient-specific equations to estimate pre-infection vertebral volumes, enabling objective bone loss assessment via the “Destruction Quotient.” This method enhances clinical decision-making by supplementing imaging with quantitative metrics. AI-driven segmentation and densitometry may further enhance accuracy and prognostic value.

Acknowledgements None.

Author contributions S.L., M.B., M.K., and V.A. conceived the study (Conceptualization).S.L., M.B., M.K., J.S., and M.S. developed the methodology.M.B., M.H., and G.N. implemented the software.S.L., M.B., J.K., and M.L. conducted validation.S.L., M.B., M.K., and J.S. performed formal analysis.S.L., M.B., J.S., J.K., S.B., and M.S. carried out the investigation.V.A., G.N., S.B., and M.L. supplied resources.M.B., J.K., M.H., M.S., G.N., and S.B. curated the data.S.L. and M.B. drafted the original manuscript.All authors (S.L., M.B., J.S., J.K., S.B., M.S., G.N., M.H., M.L., V.A., M.K.) reviewed and edited the manuscript.S.L., M.B., M.K., and M.H. prepared the visualizations.V.A., M.K., and M.L. provided supervision.S.L., M.B., and M.K. managed project administration.S.L. and M.B. contributed

equally to the project and manuscript. All authors approved the final version of the manuscript and agree to be accountable for its content.

Funding statement Open Access funding enabled and organized by Projekt DEAL. Open Access funding enabled and organized by Projekt DEAL. Open Access funding enabled and organized by Projekt DEAL. This research received no financial support from any public, commercial, or not-for-profit funding agencies.

Data availability The datasets generated and analyzed during the current study are available from the corresponding author upon reasonable request.

Declarations

Competing interests The authors declare that there are no conflicts of interest with respect to the authorship or publication of this article.

Ethical Approval and Informed Consent Statements The study was approved by the institutional ethics committee of the University Medical Center Regensburg (Reference number: 12–218_3-101). Due to the retrospective nature of the analysis of fully anonymized data, the requirement for written informed consent was waived by the committee.

References

1. Kramer A, Thavarajasingam SG, Neuhoff J, Ponniah HS, Ramsay DSC, Demetriades AK, Davies BM, Shiban E, Ringel F (2023) Epidemiological trends of pyogenic spondylodiscitis in germany: an EANS spine section study. *Scientific reports*. Nat Publishing Group 13:20225. https://doi.org/10.1038/s41598-023-47341-z
2. Heck VJ, Prasse T, Klug K, Vinas-Rios JM, Oikonomidis S, Klug A, Kernich N, Weber M, von der Höh N, Lenz M, Walter SG, Himpe B, Eysel P, Scheyerer MJ (2024) The projected increase of vertebral osteomyelitis in Germany implies a demanding challenge for future healthcare management of aging populations. Infection 52:1489–1497. https://doi.org/10.1007/s15010-024-02243-8
3. Lang S, Walter N, Schindler M, Baertl S, Szymski D, Loibl M, Alt V, Rupp M (2023) The epidemiology of spondylodiscitis in germany: A descriptive report of incidence rates, pathogens, In-Hospital mortality, and hospital stays between 2010 and 2020. J Clin Med 12:3373. https://doi.org/10.3390/jcm12103373
4. Heuer A, Strahl A, Viezens L, Koepke L-G, Stangenberg M, Dreimann M (2022) The Hamburg spondylodiscitis assessment score (HSAS) for immediate evaluation of mortality risk on hospital admission. J Clin Med 11:660. https://doi.org/10.3390/jcm11030660
5. Ziarko TP, Walter N, Schindler M, Alt V, Rupp M, Lang S (2023) Risk factors for the In-Hospital mortality in pyogenic vertebral osteomyelitis: A Cross-Sectional study on 9753 patients. Journal Clin Medicine Multidisciplinary Digit Publishing Inst 12:4805. https://doi.org/10.3390/jcm12144805
6. Kramer A, Thavarajasingam SG, Neuhoff J, Lange F, Ponniah HS, Lener S, Thomé C, Stengel FC, Fischer G, Hostettler IC, Stienen MN, Jemna M, Gousias K, Nedeljkovic A, Grujicic D, Nedeljkovic Z, Poluga J, Schär RT, Urbanski W, Sousa C, Casimiro CDO, Harmer H, Ladisich B, Matt M, Simon M, Pai D, Doenitz C, Mongardi L, Lofrese G, Buchta M, Grassner L, Trávníček P, Hosszú T, Wissels M, Bamps S, Hamouda W, Panico F, Garbossa D, Barbato M, Barbarisi M, Pantel T, Gempt J, Kasula TS, Desai S, Vitowanu JM, Rovčanin B, Omerhodzic I, Demetriades AK, Davies B, Shiban E, Ringel F (2024) Management of severe pyogenic spinal infections: the 2SICK study by the EANS spine section. Spine Journal: Official J North Am Spine Soc S1529–9430. (24)01196–3
7. Lang S, Walter N, Froemming A, Baertl S, Szymski D, Alt V, Rupp M (2023) Long-Term Patient-Related quality of life outcomes and ICD-10 symptom rating (ISR) of patients with pyogenic vertebral osteomyelitis: what is the psychological impact of this life-Threatening disease?? Eur Spine Journal: Official Publication Eur Spine Soc Eur Spinal Deformity Soc Eur Sect Cerv Spine Res Soc 32:1810–1817. https://doi.org/10.1007/s00586-023-07616-5
8. Klute L, Esser M, Henssler L, Riedl M, Schindler M, Rupp M, Alt V, Kerschbaum M, Lang S (2024) Anterior column reconstruction of destructive vertebral osteomyelitis at the thoracolumbar spine with an expandable vertebral body replacement implant: A retrospective, monocentric radiological cohort analysis of 24 cases. Journal Clin Medicine Multidisciplinary Digit Publishing Inst 13:296. https://doi.org/10.3390/jcm13010296
9. Limthongkul W, Karaikovic EE, Savage JW, Markovic A (2010) Volumetric analysis of thoracic and lumbar vertebral bodies. Spine Journal: Official J North Am Spine Soc 10:153–158. https://doi.org/10.1016/j.spinee.2009.11.018
10. Komemushi A, Tanigawa N, Kariya S, Kojima H, Shomura Y, Sawada S (2005) Percutaneous vertebroplasty for compression fracture: analysis of vertebral body volume by CT volumetry. Acta Radiol (Stockholm Sweden: 1987) 46:276–279. https://doi.org/10.1080/02841850510016072
11. Rak M, Steffen J, Meyer A, Hansen C, Tönnies K (2019) Combining convolutional neural networks and star convex cuts for fast whole spine vertebra segmentation in MRI. Comput Methods Programs Biomed 177:47–56. https://doi.org/10.1016/j.cmpb.2019.05.003
12. Hille G, Saalfeld S, Serowy S, Tönnies K (2018) Vertebral body segmentation in wide range clinical routine spine MRI data. Comput Methods Programs Biomed 155:93–99. https://doi.org/10.1016/j.cmpb.2017.12.013
13. Salaffi F, Ceccarelli L, Carotti M, Di Carlo M, Polonara G, Facchini G, Golfieri R, Giovagnoni A (2021) Differentiation between infectious spondylodiscitis versus inflammatory or degenerative spinal changes: how can magnetic resonance imaging help the clinician?? Radiol Med 126:843–859. https://doi.org/10.1007/s11547-021-01347-7
14. Jevtic V (2004) Vertebral infection. Eur Radiol Supplements 14:1–1. https://doi.org/10.1007/s00330-003-2046-x
15. Stangenberg M, Mende KC, Mohme M, Krätzig T, Viezens L, Both A, Rohde H, Dreimann M (2021) Influence of Microbiological diagnosis on the clinical course of spondylodiscitis. Infection 49:1017–1027. https://doi.org/10.1007/s15010-021-01642-5
16. 3D Slicer Image Computing Platform| 3D Slicer. https://www.slicer.org/

17. Fedorov A, Beichel R, Kalpathy-Cramer J, Finet J, Fillion-Robin J-C, Pujol S, Bauer C, Jennings D, Fennessy F, Sonka M, Buatti J, Aylward S, Miller JV, Pieper S, Kikinis R (2012) 3D slicer as an image computing platform for the quantitative imaging network. Magn Reson Imaging 30:1323–1341. https://doi.org/10.1016/j.mri.2012.05.001
18. You Y, Niu Y, Sun F, Huang S, Ding P, Wang X, Zhang X, Zhang J (2022) Three-Dimensional printing and 3D slicer powerful tools in Understanding and treating neurosurgical diseases. Front Surg 9:1030081. https://doi.org/10.3389/fsurg.2022.1030081
19. Molloy S, Mathis JM, Belkoff SM (2003) The effect of vertebral body percentage fill on mechanical behavior during percutaneous vertebroplasty. Spine 28:1549–1554
20. Odaci E, Sahin B, Sonmez OF, Kaplan S, Bas O, Bilgic S, Bek Y, Ergür H (2003) Rapid Estimation of the vertebral body volume: A combination of the Cavalieri principle and computed tomography images. Eur J Radiol 48:316–326. https://doi.org/10.1016/S0720-048X(03)00077-9
21. Komemushi A, Tanigawa N, Kariya S, Kojima H, Shomura Y, Sawada S (2005) Percutaneous Vertebroplasty for Compression Fracture: Analysis of Vertebral Body Volume by CT Volumetry. *Acta Radiologica*, Taylor & Francis. https://www.tandfonline.com/doi/abs/10.1080/02841850510016072
22. Caula A, Metmer G, Havet E (2016) Anthropometric approach to lumbar vertebral body volumes. Surg Radiologic Anatomy: SRA 38:303–308. https://doi.org/10.1007/s00276-015-1552-2
23. Schömig F, Li Z, Perka L, Vu-Han T-L, Diekhoff T, Fisher CG, Pumberger M (2022) Georg schmorl prize of the German spine society (DWG) 2021: spinal instability spondylodiscitis score (SISS)-a novel classification system for spinal instability in spontaneous spondylodiscitis. Eur Spine Journal: Official Publication Eur Spine Soc Eur Spinal Deformity Soc Eur Sect Cerv Spine Res Soc 31:1099–1106. https://doi.org/10.1007/s00586-022-07157-3
24. Egger J, Nimsky C, Chen X (2017) Vertebral body segmentation with growcut: initial experience, workflow and practical application. SAGE Open Med 5:2050312117740984. https://doi.org/10.1177/2050312117740984
25. Chen Y, Vinogradskiy Y, Yu Y, Shi W, Liu H (2022) Clinical evaluation of an Auto-Segmentation tool for spine SBRT treatment. Front Oncol 12:842579. https://doi.org/10.3389/fonc.2022.842579
26. Zhang J, Liu F, Xu J, Zhao Q, Huang C, Yu Y, Yuan H (2023) Automated detection and classification of acute vertebral body fractures using a convolutional neural network on computed tomography. Front Endocrinol 14:1132725. https://doi.org/10.3389/fendo.2023.1132725
27. Dieckmeyer M, Löffler MT, El Husseini M, Sekuboyina A, Menze B, Sollmann N, Wostrack M, Zimmer C, Baum T, Kirschke JS (2022) Level-Specific volumetric BMD threshold values for the prediction of incident vertebral fractures using opportunistic QCT: A Case-Control study. Front Endocrinol 13:882163. https://doi.org/10.3389/fendo.2022.882163
28. Widaa A, Claro T, Foster TJ, O'Brien FJ, Kerrigan SW (2012) Staphylococcus Aureus protein A plays a critical role in mediating bone destruction and bone loss in osteomyelitis. PLOS ONE Public Libr Sci 7:e40586. https://doi.org/10.1371/journal.pone.0040586
29. Cheung GYC, Bae JS, Otto M Pathogenicity and virulence of Staphylococcus Aureus. Virulence, 12, 547–569. https://doi.org/10.1080/21505594.2021.1878688
30. Burke Ó, Zeden MS, O'Gara JP (2024) The pathogenicity and virulence of the opportunistic pathogen Staphylococcus Epidermidis. Virulence 15:2359483. https://doi.org/10.1080/21505594.2024.2359483
31. Lopez J, Tatar Z, Tournadre A, Couderc M, Pereira B, Soubrier M, Dubost J-J (2017) Characteristics of spontaneous Coagulase-Negative Staphylococcal spondylodiscitis: A retrospective comparative study versus Staphylococcus Aureus spondylodiscitis. BMC Infect Dis 17:683. https://doi.org/10.1186/s12879-017-2783-0
32. Lang S, Frömming A, Walter N, Freigang V, Neumann C, Loibl M, Ehrenschwender M, Alt V, Rupp M (2021) Is there a difference in clinical features, Microbiological epidemiology and effective empiric antimicrobial therapy comparing Healthcare-Associated and Community-Acquired vertebral osteomyelitis?? *Antibiotics*. Multidisciplinary Digit Publishing Inst 10:1410. https://doi.org/10.3390/antibiotics10111410
33. Renz N, Haupenthal J, Schuetz MA, Trampuz A (2017) Hematogenous vertebral osteomyelitis associated with intravascular Device-Associated Infections - A retrospective cohort study. Diagn Microbiol Infect Dis 88:75–81. https://doi.org/10.1016/j.diagmicrobio.2017.01.020
34. Lee C-Y, Wu M-H, Cheng C-C, Huang T-J, Huang T-Y, Lee C-Y, Huang J-C, Li Y-Y (2016) Comparison of Gram-Negative and Gram-Positive hematogenous pyogenic spondylodiscitis: clinical characteristics and outcomes of treatment. BMC Infect Dis 16:735. https://doi.org/10.1186/s12879-016-2071-4
35. Kang S-J, Jang H-C, Jung S-I, Choe PG, Park WB, Kim C-J, Song K-H, Kim ES, Kim HB, Oh M, Kim NJ, Park K-H (2015) Clinical Characteristics and Risk Factors of Pyogenic Spondylitis Caused by Gram-Negative Bacteria. *PLOS ONE*, Public Library of Science, 10, e0127126. https://doi.org/10.1371/journal.pone.0127126
36. Joerger A-K, Albrecht C, Lange N, Meyer B, Wostrack M (2023) In-Hospital mortality from spondylodiscitis: insights from a Single-Center retrospective study. J Clin Med 12:7228. https://doi.org/10.3390/jcm12237228
37. Okamoto K, Nakashima T, Shinohara M, Negishi-Koga T, Komatsu N, Terashima A, Sawa S, Nitta T, Takayanagi H (2017) Osteoimmunology: the conceptual framework unifying the immune and skeletal systems. Physiol Rev 97:1295–1349. https://doi.org/10.1152/physrev.00036.2016
38. Guder C, Gravius S, Burger C, Wirtz DC, Schildberg FA (2020) Osteoimmunology: A current update of the interplay between bone and the immune system. Front Immunol 11:58. https://doi.org/10.3389/fimmu.2020.00058

Authors and Affiliations

Siegmund Lang[1] · Michael Bachtler[1] · Josina Straub[1] · Jonas Krückel[1] · Susanne Baertl[1] · Melanie Ardelt[2,3] · Gerardo Napodano[4] · Michael Haimerl[5] · Markus Loibl[6] · Volker Alt[1] · Maximilian Kerschbaum[1]

✉ Siegmund Lang
Siegmund.Lang@ukr.de

Michael Bachtler
Michael.Bachtler@stud.uni-regensburg.de

Josina Straub
Josina.Straub@ukr.de

Jonas Krückel
Jonas.Krueckel@ukr.de

Susanne Baertl
Susanne.Baertl@ukr.de

Melanie Ardelt
Schindler.Melanie@gmx.at

Gerardo Napodano
Gerardo.Napodano@ukr.de

Michael Haimerl
Michael.Haimerl@ukr.de

Markus Loibl
Markus.Loibl@kws.ch

Volker Alt
Volker.Alt@ukr.de

Maximilian Kerschbaum
Maximilian.Kerschbaum@ukr.de

1 Department of Trauma Surgery, University Medical Center Regensburg, Regensburg, Germany

2 Department of Orthopaedics and Trauma Surgery, University Hospital Krems, Karl Landsteiner University of Health Sciences, Krems, Austria

3 Danube University Krems, Krems, Austria

4 Institute of Radiology, University Hospital Regensburg, Regensburg, Germany

5 Department of Radiology, Klinikum Würzburg Mitte, Wurzburg, Germany

6 Department of Spine Surgery, Schulthess Clinic, Zurich, Switzerland